Oncogene (2018) **37**, 313–322

www.nature.com/onc

ORIGINAL ARTICLE

Endogenous androgen receptor proteomic profiling reveals genomic subcomplex involved in prostate tumorigenesis

S Stelloo[1], E Nevedomskaya[1,2], Y Kim[1,2], L Hoekman[3], OB Bleijerveld[3], T Mirza[1], LFA Wessels[2,4], WM van Weerden[5], AFM Altelaar[3,6], AM Bergman[1,7] and W Zwart[1]

Androgen receptor (AR) is a key player in prostate cancer development and progression. Here we applied immunoprecipitation mass spectrometry of endogenous AR in LNCaP cells to identify components of the AR transcriptional complex. In total, 66 known and novel AR interactors were identified in the presence of synthetic androgen, most of which were critical for AR-driven prostate cancer cell proliferation. A subset of AR interactors required for LNCaP proliferation were profiled using chromatin immunoprecipitation assays followed by sequencing, identifying distinct genomic subcomplexes of AR interaction partners. Interestingly, three major subgroups of genomic subcomplexes were identified, where selective gain of function for AR genomic action in tumorigenesis was found, dictated by FOXA1 and HOXB13. In summary, by combining proteomic and genomic approaches we reveal subclasses of AR transcriptional complexes, differentiating normal AR behavior from the oncogenic state. In this process, the expression of AR interactors has key roles by reprogramming the AR cistrome and interactome in a genomic location-specific manner.

Oncogene (2018) **37,** 313–322; doi:10.1038/onc.2017.330; published online 18 September 2017

INTRODUCTION

The androgen receptor (AR) is a member of the nuclear receptor superfamily of ligand-activated transcription factors (TFs). Exposure of prostate cancer cells to androgens leads to AR nuclear translocation where it interacts with the chromatin to regulate transcriptional programs involved in prostate cancer cell proliferation.[1]

Over the past decades, numerous reports have greatly increased our understanding of AR function, along with the identification of coregulators involved in these processes. Upon ligand activation, AR recruits a multitude of regulatory proteins acting in concert with AR to transduce the hormonal signal. These regulatory proteins, so called coactivators and corepressors, can modify AR action by either enhancing or inhibiting gene transcription.[2] To date, >300 AR-interacting proteins have been reported to modulate AR transcriptional activity by several diverse mechanisms.

A specific subgroup of AR coregulators, including ATP/dependent nucleosome remodeling proteins (for example, BRG1) and pioneer factors (for example, FOXA1), affect gene activation through their ability to remodel the chromatin, facilitating AR binding, complex formation and transcriptional activity.[3,4] Genome-wide selective action of pioneer factors dictates AR binding at distinct sites,[5] of which the vast majority are enhancer regions hallmarked by the histone modifications H3K27ac and H3K4me1.[6–8] Other coregulators influence AR functionality via posttranslational modifications of AR itself, such as acetylation, phosphorylation, sumoylation and ubiquitination.[9]

Several coregulators of AR are subjected to transcriptional regulation by androgens themselves, and in turn, these proteins regulate AR transcriptional activity providing an intricate feedback mechanism. HOXB13, for instance, is transcriptionally regulated by androgens[10] and physically interacts with the AR to modulate its activity.[11,12] Interaction of HOXB13 with AR enhances AR recruitment to binding sites containing HOX regulatory elements.[11,13] The fact that other TFs influence AR signaling and recruitment to the DNA yields new opportunities for therapeutic intervention. This notion is further strengthened through recent work by us and others revealing that AR chromatin binding is significantly changed during prostate cancer progression.[13–15] Agents targeting these TFs required for AR action are in various stages of preclinical or clinical evaluation, including Olaparib (PARP1 inhibitor),[16] JQ1 (BRD4 inhibitor)[17] and NCL1 (LSD1 inhibitor).[18]

Given the prominent role of AR coregulators in mediating AR transcriptional activity, it is key to systematically interrogate the total protein interactome of the AR in prostate cancer cells. Most methodologies to expand the AR interactome so far involve exogenous-tagged AR or *in vitro* AR binding to DNA templates.[19–25] Here we performed endogenous purification of AR transcriptional complexes and generated genome-wide binding maps of its interactors in LNCaP prostate cancer cells. Integration of proteomic and genomic data revealed distinct AR transcriptional subcomplexes on a genome-wide scale directly influencing AR transcriptional programs. Assessment of the most differential binding sites among all studied coregulators reveals a previously identified dependence and reprogramming of AR by

[1]Division of Oncogenomics, The Netherlands Cancer Institute, Amsterdam, The Netherlands; [2]Division of Molecular Carcinogenesis, The Netherlands Cancer Institute, Amsterdam, The Netherlands; [3]Mass Spectrometry and Proteomics Facility, The Netherlands Cancer Institute, Amsterdam, The Netherlands; [4]Faculty of EEMCS, Delft University of Technology, Delft, The Netherlands; [5]Department of Urology, Erasmus MC Cancer Institute, Erasmus University Medical Center, Rotterdam, The Netherlands; [6]Biomolecular Mass Spectrometry and Proteomics Group, Bijvoet Center for Biomolecular Research and Utrecht Institute for Pharmaceutical Sciences, The Netherlands Proteomics Centre, Utrecht University, Utrecht, The Netherlands and [7]Division of Medical Oncology, The Netherlands Cancer Institute, Amsterdam, The Netherlands. Correspondence: Dr W Zwart or S Stelloo, Division of Oncogenomics, The Netherlands Cancer Institute, Plesmanlaan 121, Amsterdam 1066cx, The Netherlands.
E-mail: w.zwart@nki.nl or s.stelloo@nki.nl
Received 8 March 2017; revised 10 July 2017; accepted 6 August 2017; published online 18 September 2017

FOXA1 and HOXB13,[13] which affect epigenetic rewiring required for cell transformation and prostate tumorigenesis.

RESULTS

Identification of the AR interactome

To identify cooperating factors that are involved in the regulation of AR signaling, we used an unbiased proteomic approach RIME (Rapid Immunoprecipitation Mass Spectrometry of Endogenous proteins).[26] The RIME method combines precipitation of endogenous protein complexes, from crosslinked and sheared chromatin preparations, with mass spectrometry analysis.

Hormone-deprived LNCaP cells were stimulated for 4 h with synthetic androgen R1881 followed by immunoprecipitation of endogenous AR, in three independent biological replicates. After applying label-free quantitation of mass spectrometry data, a total of 316 proteins were identified as co-purified together with AR, of which 66 proteins were being quantitatively enriched over the negative control (immunoglobulin G (IgG)) (Figure 1, Supplementary Figure S1). A full list of AR-interacting proteins is provided in Supplementary Table 1. The identified AR interaction partners are involved in different molecular functions, such as DNA repair, chromatin remodeling, transcriptional repression and cell cycle (Figure 1a). Peptide coverage of selected AR-associated proteins is shown in Figure 1b. AR was detected with almost 30% peptide coverage of amino-acid residues. The selected interacting proteins were validated by co-immunoprecipitation experiments using the chromatin fraction followed by western blotting analysis in two prostate cancer cell lines: LNCaP and LAPC4 (Figure 1c). In both cell lines, we confirmed interaction of AR with known interactors (ARID1a, HOXB13, HSP90, FOXA1, PARP1) as well as novel AR interactors (TLE3 and TRIM28). Even though FOXA1 was identified as AR interactor based on AR RIME, no statistically significant enrichment over IgG was observed (Supplementary Figure S1). Co-immunoprecipitation did validate FOXA1 as AR interactor in our analyses, implying a level of false negativity using this approach. All validated interactors are enriched in the chromatin-bound AR complex, with exception of HSP90, which is known to dissociate from AR upon hormone stimulation.[27] Furthermore, AR interactions with ARID1a, BRG1, TLE3, PARP1, RCC1 and FOXA1 were further verified by co-immunoprecipitation on tissue derived from two independent prostate cancer patient-derived xenograft (PDX) models (Figure 1d).

In summary, using endogenous immunoprecipitation of the AR coupled with mass spectrometry, we identified ligand-dependent known and novel AR interactors in LNCaP prostate cancer cells.

AR interactors are essential for prostate cancer cell proliferation

As AR is critically involved in prostate cancer cell growth, AR-interacting proteins are expected to have an impact on cell proliferation as well. To identify AR interactors whose loss affects cell growth, we analyzed data from the Broad Institute's Project Achilles. The Project Achilles data scored the effect of $>19\,000$ CRISPR/Cas9-mediated individual gene knockout on cell proliferation (ATARiS score) in 33 cancer cell lines. Two prostate cancer cell lines were studied, one AR-positive cell line LNCaP and an AR-negative cell line PC3. Figures 2a–f show waterfall plots with the ATARiS score for each significant AR interactor, ranked by phenotype score in LNCaP cells. AR itself scored as top essential gene for LNCaP cell growth, among all AR interactors (Figure 2a). As expected, growth of PC3 cells was not affected by AR knockout (Figure 2b, first bar). Furthermore, knockout of many AR interactors in LNCaP cells reduced cell growth, as represented by a greater shift of the waterfall to the left (P-value < 0.001) (Figure 2a). The AR interactors showed significantly different effects on LNCaP cell proliferation as compared with other cell types (Figure 2, P-values are listed in Supplementary Table 2).

As an independent biological validation series, we made use of another genome-wide CRISPR screen for essential genes in LNCaP cells cultured in the presence of dihydrotestosterone.[28] We investigated the ranking of the AR interactors in the screen by calculating the mean robust rank aggregation (RRA) score, in which a low RRA score indicates essentiality for LNCaP growth. The mean RRA score (0.25) of the AR interactors demonstrates essentiality for LNCaP growth in this independent CRISPR screen, as compared with 1000 bootstrapped RRA score means (95% confidence interval 0.28–0.43) (Supplementary Figure 2A).

AR interactors do not have a consistent similar effect across all cell lines, as no effect was observed in averaged signal of all 33 cell lines tested (Figure 2c), nor in specific other types of cancer such as pancreas (Figure 2d), breast (Figure 2e) and skin (Figure 2f).

Genome-wide mapping of AR interactors

Having characterized the AR interactome that is essential for LNCaP proliferation, we next generated genome-wide chromatin-binding profiles of AR and its interactors with different molecular functions to reconstruct the AR transcriptional complex. We performed chromatin immunoprecipitation assays followed by sequencing (ChIP-seq) in LNCaP cells for AR, ARID1a, BRG1, FOXA1, HOXB13, TLE3, TRIM28 and WDHD1, all shown to be required for LNCaP proliferation (Figure 2 and Supplementary Figure 2B). The cells were exposed to vehicle or R1881 in order to evaluate whether the increased interaction observed in Figure 1c can be explained by hormone-induced AR chromatin binding at sites preoccupied by the coregulators and/or due to AR-driven coregulator recruitment. Replicate experiments were performed and peaks present in at least two replicates were considered for further analysis (Supplementary Figure 3). For all seven factors, distinct peaks could be observed and shared with AR, as exemplified at four genomic locations (Figure 3a). To investigate whether the factors bind DNA directly in a sequence-specific manner or indirectly through tethering, we searched in each ChIP-seq peakset of each factor for known DNA-binding motifs (Supplementary Table 3). Motif discovery analysis for AR peaks showed strong enrichment for the androgen response element as well as sequence motifs of previously reported collaborative factors, including motifs for Forkhead, GATA and Ets factors (Figure 3b).[29–31] The androgen response element was also significantly enriched at peaks for ARID1a, BRG1 and TLE3. Motif analysis on HOXB13- and FOXA1-binding sites revealed presence of their canonical binding motifs, the homeodomain and forkhead motifs, respectively. TLE3-binding sites reveal comparable motif enrichments as HOXB13- and FOXA1-binding sites, which were expected as TLE3 chromatin recruitment is dependent on FOXA1.[32] TRIM28 regions show enrichment for motifs of the GATA domain family and the expected zinc finger family as TRIM28 is known to tether to the DNA by Krüppel-associated box zinc finger proteins.[33,34] ARID1a-, BRG1- and WDHD1-occupied sites show a variety of binding motifs, suggesting recruitment to the genome through other TFs.

By combining all peaksets, we identified 68 791 sites bound by at least 1 of the 8 TFs for both replicates in LNCaP cells across vehicle and R1881-stimulated conditions (Figure 3c). Around one-third of those peaks are bound by AR (cluster I: 26 510 peaks, Figure 3c), while the remaining sites were devoid of AR signal (cluster II: 42 281 peaks). The AR occupied cluster I sites show accessible chromatin (DNase I hypersensitivity) and presence of active histone marks (H3K27ac and H3K4 methylation) as well as RNA polymerase II signal. In contrast, cluster II displays reduced DNase I hypersensitivity signal and low RNA polymerase II signal, which was accompanied by low signal of all active histone marks tested, as compared with cluster I. Upon R1881 stimulation, chromatin binding of ARID1a, BRG1, FOXA1 and HOXB13 was

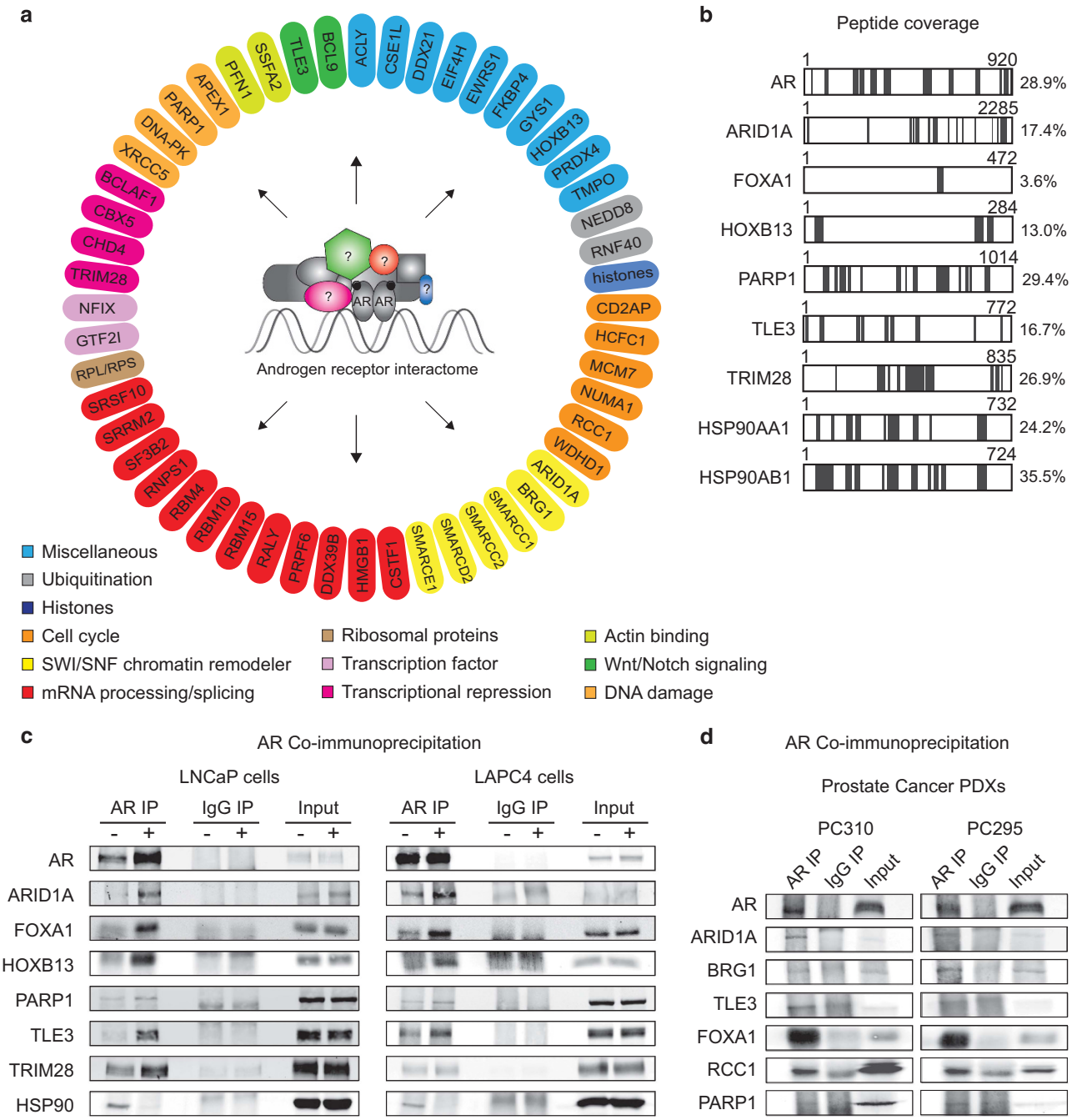

Figure 1. Purification of endogenous AR complexes. (**a**) AR-interacting proteins identified by RIME. Proteins significantly enriched over the negative control (IgG RIME) across three biological replicates are shown. Proteins are colored according to molecular function. (**b**) Peptide coverage for AR and selected AR-associated proteins. The identified peptides are colored in gray. (**c**) Validation of AR-associated proteins with co-immunoprecipitation in LNCaP (left) and LAPC4 (right) cells treated with vehicle (−) or R1881 (+). IgG served as a negative control. The western blots are representative of two biological replicates. (**d**) AR co-immunoprecipitation in prostate cancer PDX tissue, with IgG as negative control.

increased at AR-occupied sites, while the other factors TLE3, TRIM28 and WDHD1 are not affected by R1881 treatment (Figure 3d, cluster I). The 42 281 sites from cluster II showed absence of AR binding but did display evident signal for HOXB13 and FOXA1, which was not affected by R1881 treatment (Figure 3d). Interestingly, while devoid of AR, TRIM28 and TLE3 signal in cluster II decreased upon R1881 stimulation (Figures 3c and d). Sites from clusters I and II have similar genomic distributions with most enrichment in intron and distal intergenic regions (Figure 3e).

Cumulatively, all tested AR interactors, as identified by RIME and confirmed by co-immunoprecipitation, interacted with AR in a chromatin-bound state, of which a subset were R1881 induced (ARID1A, BRG1, FOXA1, HOXB13) while others were found at AR sites independent of R1881 stimulation (TLE3, TRIM28, WDHD1).

Acquired transcriptional AR subcomplexes in prostate carcinogenesis

In total, 26 510 AR-binding sites were found in LNCaP cells (Figure 3c; cluster I), though the composition of the transcriptional

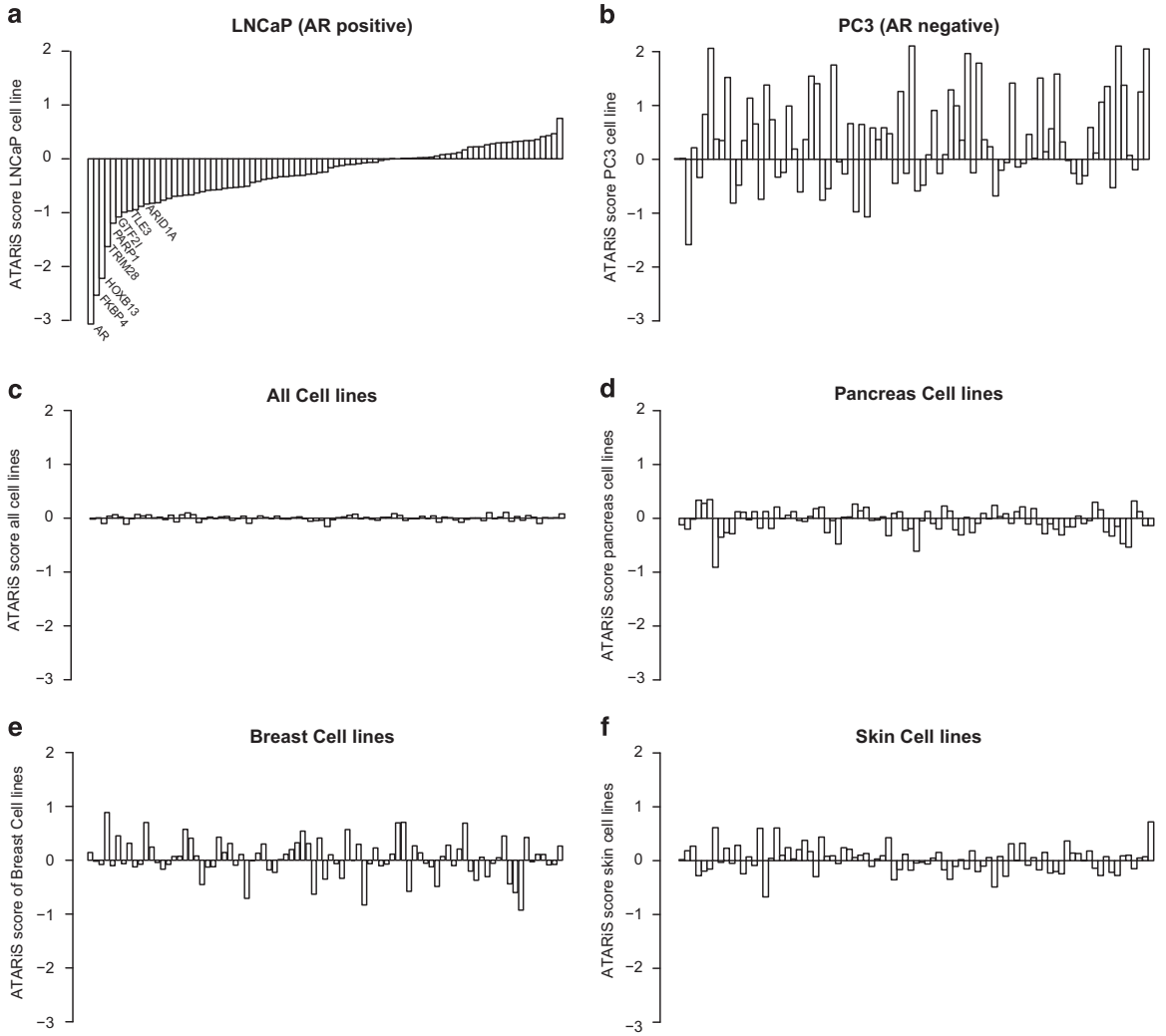

Figure 2. AR interactors are essential for prostate cancer cell proliferation. (**a**) ATARiS gene level scores for AR interactors were ranked by phenotype score in LNCaP cells. A negative ATARiS score indicates decreased cell proliferation/survival in the knockout cells. (**b**–**f**) ATARiS score for each significant AR interactor, maintaining the order as in LNCaP cells (**a**), but using ATARiS scores from PC3 cells (**b**), all cancer cell types (**c**), pancreas (**d**), breast (**e**) or skin (**f**) cancer cell lines.

complex may differ between different genomic locations. Therefore, we next analyzed the ChIP-seq data of all 8 interactors, including AR, to determine whether quantitative differences could be identified in relative binding between factors in cluster I. Using read count in the peaks of cluster I, the eight TFs were clearly separated based on principal component analysis reflecting two major groups (Figure 4a). One group encompasses FOXA1, HOXB13 and TLE3 while the other comprises of AR, BRG1, TRIM28 and WDHD1. For further analysis, we focused on the top 2000 regions (Supplementary Table 4) with the most variable binding of the TFs at AR sites revealing three distinct clusters upon hierarchical clustering (Figure 4b). Cluster 1.1 comprises 1151 peaks with a strong signal for FOXA1, HOXB13 and TLE3, while cluster 1.2 is depleted for these factors. The third cluster 1.3 is characterized by strong signal for AR and FOXA1, with very weak signal for HOXB13. As the binding of the sequence-specific TFs (FOXA1, HOXB13 and AR) is quantitatively divergent between the three clusters, we performed motif enrichment analysis to test whether their binding preference is due to underlying DNA sequence. Motif enrichment is highly consistent with the observed TF binding (Figures 4b and c) where cluster 1.1 (exposing strong FOXA1 and HOXB13 signal) has both forkhead and homeodomain motifs, whereas these motifs were not significantly enriched in regions from cluster 1.2. In addition, lack of enrichment for homeodomain motifs in cluster 1.3 is in concordance with lack of HOXB13 binding at these regions, while forkhead motifs as well as FOXA1 binding were observed (Figure 4c, green).

As AR sites in cluster 1.1 are shared with HOXB13 and FOXA1 sites, the question arose whether AR binding at these regions depends on the presence of these TFs. For this, we used publicly available data on AR-expressing normal prostate epithelium cells (LHSAR), where AR ChIP-seq was performed with or without the overexpression of FOXA1 and/or HOXB13 (GSE56288).[13] Although no AR binding was found at sites from cluster 1.1 in the absence of FOXA1 and HOXB13 expression in LHSAR cells, overexpression of either of these two TFs sufficed in inducing AR binding at these sites (Figures 4d and e). In addition, FOXA1 overexpression (but not HOXB13) enhanced AR recruitment at the sites of cluster 1.3, where only forkhead motifs were found enriched (Figures 4d and e (green)). Gained AR signal at clusters 1.1 and 1.3, observed after exogenous introduction of HOXB13/FOXA1 or FOXA1 alone, respectively, was at the expense of the sites of cluster 1.2 where AR signal was found decreased, suggesting a competitive relocation of AR in this setting (Figures 4d and e (red)).

Does relocation of AR to clusters 1.1 and 1.3 by overexpression of FOXA1 and/or HOXB13 coincide with altered expression of

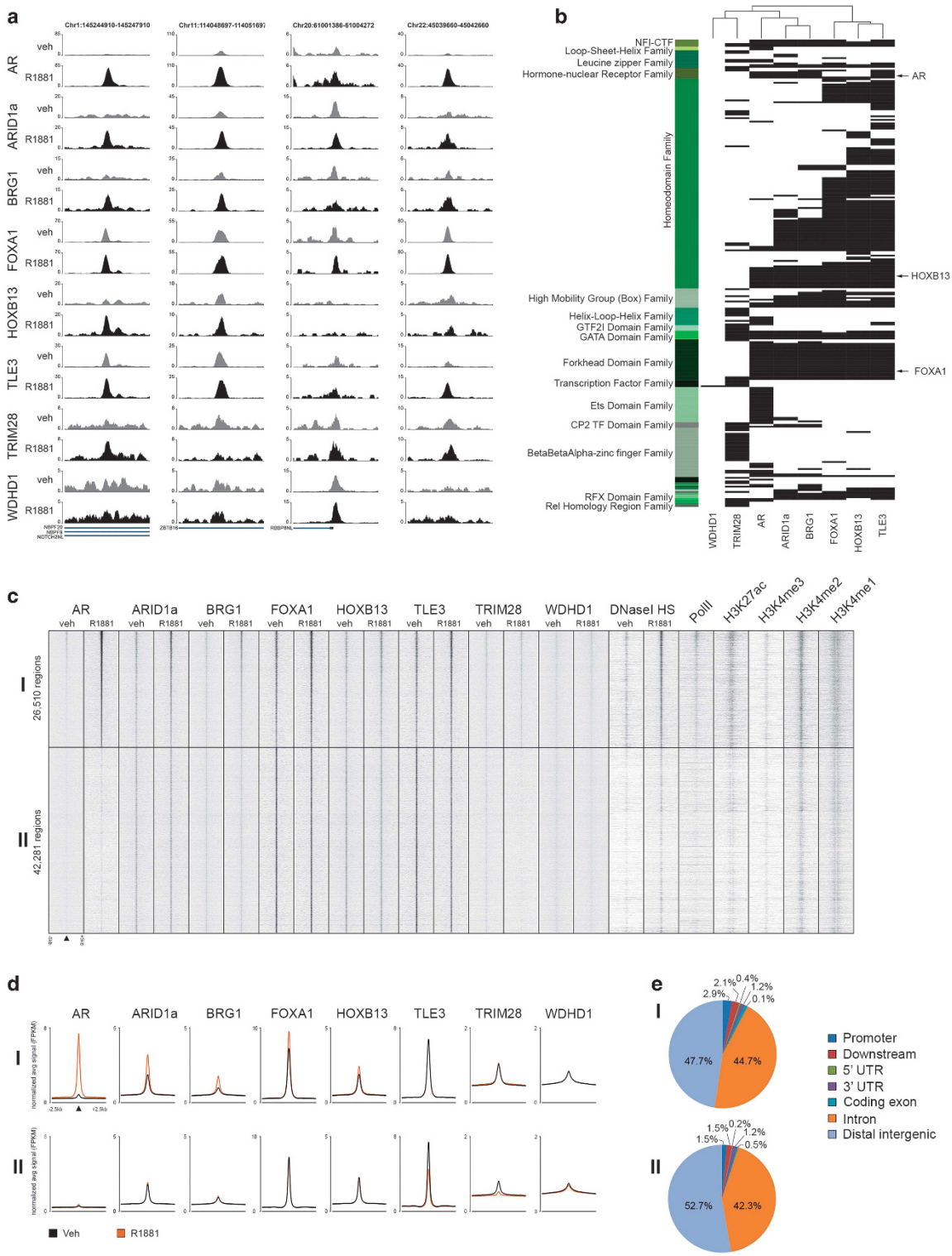

Figure 3. Genome-wide mapping of AR and its interactors. (**a**) Snapshots for AR, ARID1a, BRG1, FOXA1, HOXB13, TLE3, TRIM28 and WDHD1 ChIP-seq are shown across four example loci for vehicle (gray) and R1881 (black) conditions. Genomic coordinates are indicated. (**b**) Enrichment of motifs in each ChIP-seq peakset. Each row of the heatmap represents a motif that is significantly enriched in at least one ChIP-seq peakset. Motifs significantly enriched in the peaksets are indicated in black. (**c**) Heatmap showing ChIP-seq signal (fragments per kilobase pair per million reads (FPKM)) in vehicle or R1881 conditions for AR, ARID1a, BRG1, FOXA1, HOXB13, TLE3, TRIM28 and WDHD1 as well as DNase I hypersensitivity, RNA Pol II and histone marks, including H3K27ac and H3K4 monomethylation, dimethylation and trimethylation from publicly available data sets (Supplementary Table 9 for references and GEO accession numbers). Regions are sorted according to decreasing signal in AR binding. Data are centered at TF peaks, depicting a 5-kb window around the peak. (**d**) Average signal (FPKM) for ChIP-seq data sets at AR-occupied regions (cluster I) and non-AR-occupied sites (cluster II). Data are centered at TF peaks, depicting a 2.5-kb window around the peak. Vehicle-stimulated samples are shown in black and R1881 stimulation in orange. (**e**) Genomic distribution of peaks from cluster I: AR-occupied sites (top) and cluster II: non-AR sites (bottom) across genomic features.

proximal genes? To address this, RNA-seq data from the LHSAR cells with or without overexpression of FOXA1 and/or HOXB13 was analyzed. All genes with a proximal AR site were considered (list of genes is provided in Supplementary Table 5). We used a hypergeometric test to determine the degree of overrepresentation of the AR target genes from each cluster within the list of differentially expressed genes (comparing cells transduced with *LacZ* control to cells overexpressing FOXA1, HOXB13 or both) (Supplementary Table 6). Strikingly, genes from cluster 1.1 show a significant overlap with the differentially expressed genes upon overexpression of both FOXA1 and HOXB13. No significant overlap of genes from cluster 1.2 was found upon FOXA1 or HOXB13 overexpression, in line with the observed absence of the corresponding sequence motifs (Figure 4c). However, genes from cluster 1.3 were not significantly affected by HOXB13 overexpression, while this was the case when FOXA1 was overexpressed.

AR-expressing normal prostate epithelial LHSAR cells illustrate redirecting of AR to regions of clusters 1.1 and 1.3 when cells overexpress FOXA1 and HOXB13, resembling an AR-binding profile as observed in the prostate cancer cells LNCaP (Figure 4b). Therefore, we next tested whether AR binding in clusters 1.1 and 1.3 were gained in human prostate tumors ($n = 13$), as compared with normal prostate tissue ($n = 7$).[13] In binding sites from clusters 1.1 and 1.3, AR signal was stronger in tumor tissue as compared with normal prostate tissue, while AR signal in cluster 1.2 was comparable between both states (Figures 4f and g). This illustrates that genome-wide mapping of AR interactors can discriminate between 'AR sites found in normal epithelial cells' and 'tumor-associated AR sites'. Furthermore, the expression of FOXA1 and HOXB13 is significantly increased in tumors as compared with normal prostate tissue while AR remained unaltered (Supplementary Figure 4). This further corroborates the observations that FOXA1 and HOXB13 expression can dictate AR binding as seen in the normal prostate epithelial LHSAR cells.

To test whether genes with proximal AR sites (< 20 kb from transcription start site or gene body) are differentially expressed between normal and tumor tissue, we conducted differential expression analysis using The Cancer Genome Atlas gene expression data set consisting of 496 prostate tumor samples and 53 normal prostate samples (downloaded from https://xenabrowser.net/). Even though genes from all three clusters were significantly enriched in the differentially expressed gene list between normal and tumor tissue, larger fold enrichment was found for genes from cluster 1.1 (2.74 versus 1.62 and 1.84 for clusters 1.2 and 1.3, respectively; Supplementary Table 7). Cumulatively, our results indicate that AR binding to the chromatin is tightly regulated by other TFs, with the identification of various subcomplexes on a genome-wide scale. Differential involvement of interacting transcriptional regulators as part of the AR complex directly influences AR transcriptional programs. Our results, consistent with an earlier study,[13] suggest that alterations in the expression of AR-interacting TFs FOXA1 and HOXB13 reprograms AR binding and affects epigenetic rewiring required for transformation and prostate tumorigenesis.

DISCUSSION

AR has a critical role in prostate cancer development and progression. Along with the altered biological state of the tissue during tumorigenesis, massive changes in epigenetic state and AR cistrome are observed.[13–15] As the AR cistrome is under the direct control of a number of its interaction partners, alterations in AR protein complex composition may have direct clinical implications. Hence, we used an unbiased proteomic approach to identify endogenous AR transcription regulatory complexes, revealing AR interactions with several groups of functionally related proteins (Figure 1). In line with prior work that functionally links AR action with DNA damage induction,[35–39] multiple DNA damage repair proteins were identified, including PARP1, DNA-PK and APEX1. Furthermore, members of the chromatin remodeling SWI/SNF complex were found, known to interact with AR to reorganize the chromatin upon activation.[40] In accordance with these results, BRG1 was recruited to AR sites upon R1881 treatment as observed at regions from cluster 1 (Figure 3c and d), hallmarked by increased DNAse I hypersensitivity. Other members of the AR interactome are involved in transcriptional repression (CHD4 and HP1a) and general transcription (GTF2I and NFIX). Furthermore, multiple factors involved in mRNA processing/splicing were identified. Recent reports describe chromatin-associated proteins to directly interact with RNA, influencing transcription and chromatin-mediated posttranscriptional regulation of RNA.[41–43] Of this group, PRPF6, HMGB1 and DDX39 have been found previously to interact with AR, augmenting transcriptional activity by AR.[44–47] Other previously reported AR coactivators were found, including TRIM28/TIF1 beta,[48] which was reported previously as direct interaction partner for multiple nuclear receptors.[49] Many other well-known AR interactors, such as SRC3[50] and GATA2[30] were not detected, which may be due to low abundance, poor signal detection by mass spectrometry or poor tryptic digestion, whereas others may be false positive hits due to their high abundance (for example, ribosomal proteins).

Using a publicly available CRISPR screen, we found AR interactors strongly associated with proliferative potential in LNCaP cells, while knockout of the AR interactors did not affect proliferation of most other cell lines studied. Even for the AR/estrogen receptor-α (ERα)-positive breast cancer cell line T47D, no deviation of the median was found when knocking out the identified AR interactors, while proliferative effects were expected given that both LNCaP and T47D are hormone-driven cell lines. As, to date, no ERα RIME or AR RIME data for T47D cells has been generated, the question remains whether the AR/ERα interactome are overlapping between prostate and breast cells.

To identify any potential subcompartmentalization of AR complexes on a genome-wide scale, proteomics was followed by ChIP-seq to reveal co-occupancy of AR with its interactors at the level of individual AR-binding sites. In this study, we performed ChIP-seq for seven interactors with different molecular functions: chromatin remodelers of the SWI/SNF complex ARID1a and BRG1, pioneer TF FOXA1 and HOXB13, transcriptional coregulators TLE3 and TRIM28, and the replication initiation factor WDHD1. Although we generated ChIP-seq for a limited number of AR interactors, differential involvement of the interacting transcriptional regulators was found on a genome-wide scale. Importantly, our analyses enabled the stratification of 'AR sites found in normal epithelial cells' over 'tumor-associated AR sites', strictly based on quantitative differences in coregulator recruitment. As 'tumor-associated AR sites' were gained in the prostate cancer cell line LNCaP as well as tumor specimens as compared with normal epithelial cells (LHSAR cells and normal tissues), AR genomic action in prostate cancer may be considered as a gain-of-function phenomenon, dictated by FOXA1 and HOXB13. Altered expression of these two TFs may be an early oncogenic event that effectively increases the AR cistromic repertoire found in prostate cancer, as both FOXA1 and HOBX13 were found overexpressed in prostate tumors as compared with normal tissue (Supplementary Figure 4). Even though FOXA1/HOXB13 overexpression reprograms AR binding, R1881 treatment of exogenously AR-expressing LHSAR cells inhibits cell proliferation (data not shown).[51] Therefore, it currently remains to be determined whether additional events beyond FOXA1 and HOXB13 are required to render AR a driver in prostate carcinogenesis.

The effect of FOXA1 on the AR cistrome reported here is in full concordance with previous reports, where knockdown of FOXA1 results in extensive redistribution of AR chromatin binding.[7,52,53]

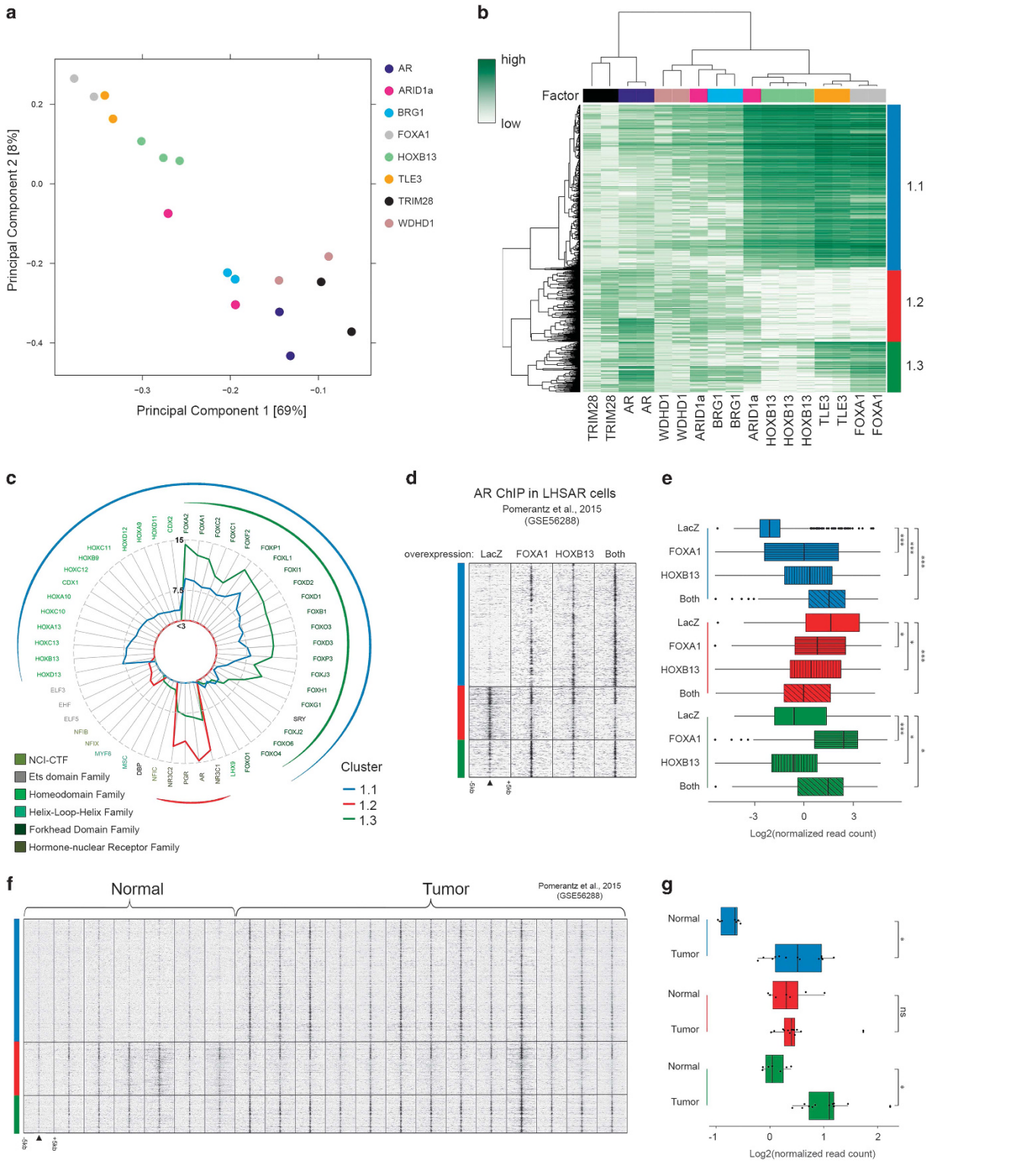

Figure 4. Distinct subsets of the AR transcriptional complexes reveal clusters associated with prostate carcinogenesis. (**a**) Principal component analysis scores plot based on the read counts of each TF under R1881 conditions in AR-binding sites. (**b**) Heatmap of the top 2000 regions with the most variable binding of the indicated TFs at AR sites. Three clusters were defined on the basis of hierarchical clustering. (**c**) Radar plot showing motif enrichment in the top 2000 variable regions (separated in the three clusters). Lengths of radii represent the absolute *Z*-score. Motif colors correspond to TF families. (**d**) Heatmap showing AR ChIP-seq signal (FPKM) in three clusters in LHSAR cells transduced with *LacZ* control, FOXA1, HOXB13 or both. Data are centered at AR peaks, depicting a 5-kb window around the peak. (**e**) Boxplot visualizing normalized AR signal (FPKM) at AR-binding sites from cluster 1.1 (blue), 1.2 (red) and 1.3 (green). $*P < 0.05$, $***P < 1e-16$ (*t*-test). (**f**) Heatmap showing AR ChIP-seq signal (FPKM) at sites of cluster 1.1 (blue),1.2 (red) and 1.3 (green) in 7 normal prostates and 13 prostate tumors. Data are centered at AR peaks, depicting a 5-kb window around the peak. (**g**) Boxplot visualizing normalized average AR signal (FPKM) at AR-binding sites from cluster 1.1 (blue), 1.2 (red) and 1.3 (green) in normal prostate tissue samples and prostate tumor samples. $*P < 0.05$ (*t*-test); NS, not significant.

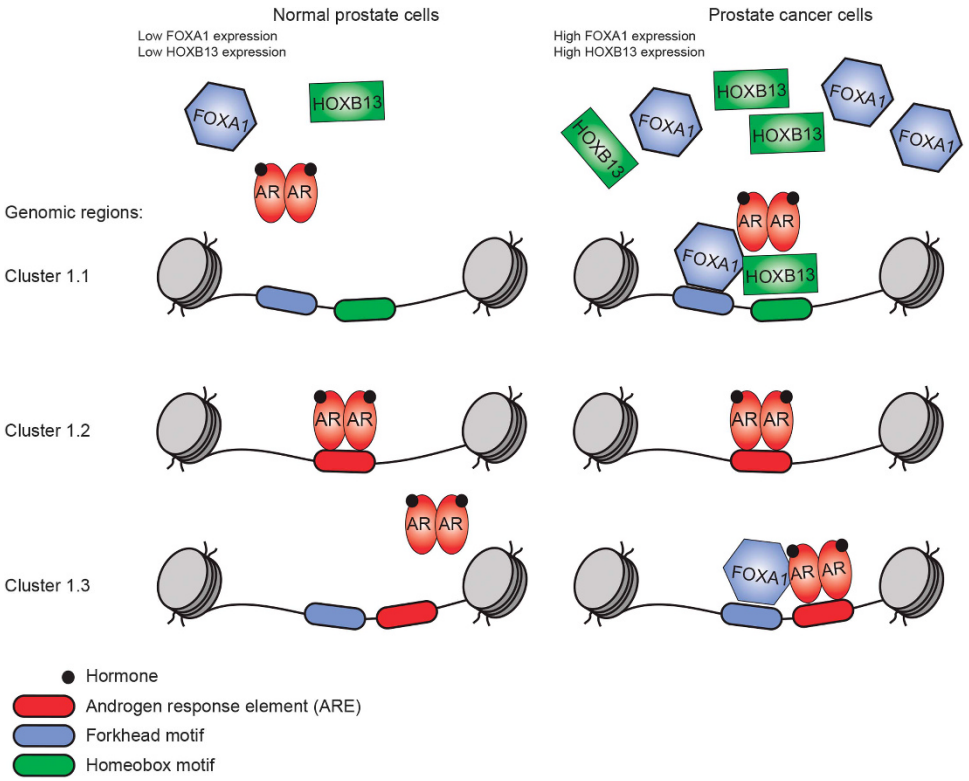

Figure 5. Model of FOXA1 and HOXB13 regulation of AR chromatin binding. Normal prostate epithelial cells have low expression of FOXA1 and HOXB13. Owing to the limiting expression of FOXA1 and HOXB13, AR binding is more prominent on genomic regions containing AREs lacking the forkhead and homeodomain motifs, whereas tumor cells have high expression of FOXA1 and HOXB13, resulting in the redistribution of AR to genomic regions containing forkhead and homeodomain motifs.

Also consistent with our observation is that HOXB13 preferably facilitates AR recruitment to binding sites containing HOX regulatory elements (Figure 4; cluster 1.1).[11] FOXA1/HOXB13/AR sites were co-occupied by TLE3 (Figure 4b), a previously reported interactor of FOXA1.[32] As TLE3 was essential for LNCaP cell proliferation (Figure 2a), cellular reprogramming in prostate cancer tumorigenesis may require other AR interactors beyond FOXA1 and HOXB13 alone. Unraveling functional involvement of the full AR interactome in tumor-specific AR sites may lead to the identification of novel therapeutic targets in the treatment of prostate cancer, with potentially limited effects on healthy tissue.

In summary, by combining proteomic and genomic approaches we provide evidence for AR subcomplex formation, differentiating normal AR behavior from the tumor state. In this process, TFs FOXA1 and HOXB13 have key roles by redirecting AR chromatin binding depending on their abundance (Figure 5) and therefore reprogram androgen-dependent AR target gene expression in prostate tumorigenesis. Understanding deviations in AR transcription complex formation between healthy and tumors cells may further aid in design of novel therapeutic intervention strategies.

MATERIALS AND METHODS

Cells

LNCaP cells were cultured in RPMI-1640 medium supplemented with 10% fetal bovine serum (FBS) and LAPC4 cells were grown in Iscove's Modified Dulbecco's Medium supplemented with 10% FBS and 1 nM R1881. For hormone depletion, cells were grown in medium containing 10% charcoal-treated FBS for 3 days. Cell lines were authenticated by STR profiling (BaseClear, Leiden, The Netherlands) and tested for mycoplasma contamination.

Patient-derived xenograft propagation

PDX-PC310 was obtained from primary prostate tumor and PDX-PC295 from a regional lymph node metastasis of otherwise untreated prostate cancer patients. Androgen-dependent PDXs were established subcutaneously in athymic male nude mice supplemented with testosterone-containing implants[54] and propagated *in vivo* as described.[55] With each mouse passage, tumors are retrieved from host animals and cut in small fragments. Fragments are transplanted subcutaneously in both shoulders of recipient 6–8-week-old male athymic NMRI nu/nu mice (Taconic, Ry, Denmark). Mice are supplemented with silastic implants containing crystalline testosterone for maximal take rates.[56] With each mouse passage, tumor fragments are formalin fixed and paraffin embedded for histological verification and remaining tumor tissue is snap-frozen. The animal protocol is conducted in accordance to the Animal Experiments Committee under the Dutch Experiments on Animals Act in adherence of the European Convention for Protection of Vertebrate Animals used for Experimental Purposes (Directive 2010/63/EU).

Rapid immunoprecipitation mass spectrometry of endogenous proteins

Cells were hormone deprived for 3 days followed by the addition of 10^{-8} M R1881 for 4 h. Cells were fixed, lysed and sonicated as previously described.[26] The nuclear lysate was incubated with 100 µl magnetic beads prebound with 10 µg AR antibody (sc-816, Santa Cruz Biotechnology, Santa Cruz, CA, USA) or rabbit IgG control (sc-2027, Santa Cruz Biotechnology). Peptide mixtures were prepared as previously described[26] and analyzed by nanoLC-MS/MS on an Orbitrap Fusion Tribrid mass spectrometer equipped with a Proxeon nLC1000 system.[57] Samples were directly loaded onto the analytical column; solvent A was 0.1% formic acid/water and solvent B was 0.1% formic acid/acetonitrile. Peptides (25% of total digest) were eluted from the analytical column at a constant flow of 250 nl/min in a 65-min gradient, containing a 46-min linear increase from 8% to 38% solvent B, followed by a 19-min wash at 100% solvent B. For mass spectrometry data analysis, see Supplementary Materials and Methods.

Co-immunoprecipitations

Cells were hormone deprived for 3 days followed by the addition of vehicle or 10^{-8} M R1881 for 4 h. Nuclear lysate was extracted as described above (RIME). The nuclear lysate was incubated with 40 µl magnetic beads prebound with 4 µg AR antibody or rabbit IgG control. At least two biological replicates were performed. After overnight immunoprecipitation, beads were washed 10 times with RIPA buffer and once with Tris-buffered saline. Beads were resuspended in Laemmli buffer and boiled at 99 °C for 15 min. Co-immunoprecipitations on PDX tissue were performed with the same method with minor modifications. Tissues were cryosectioned and fixed with 1% formaldehyde for 20 min. Tissues were homogenized and nuclear lysate was extracted. The lysate was incubated with 100 µl magnetic beads prebound with 10 µg AR antibody or rabbit IgG control. The antibodies used for western blotting are listed in Supplementary Table 8. Immunoprecipitations were carried out in at least two independent biological replicates.

Genome-wide CRISPR data

We used Achilles v3.38 data (http://vcancerportal05.broadinstitute.org/achilles/datasets/all), a data set containing scores (ATARiS score) on the impact of knockouts on the proliferation of 33 cancer cell lines. The ATARiS score for each significant AR interactor was extracted (85 values) for LNCaP and PC3 cells or averaged across all cell lines, all pancreas, breast or skin cancer cell lines. The interactors were ranked on phenotype score in LNCaP cells. Wilcoxon rank test was used to measure the difference of gene effect between LNCaP cells and other cell lines.

For the second genome-wide CRISPR screen in LNCaP cells, we used the RRA scores reported.[28] For both CRISPR screens, random sampling was performed using 1000 iterations, and the mean for each random sample (mean ATARiS score or mean RRA score) was calculated. The *P*-value was determined as the portion of random samples with a mean lower than or equal to the mean of the significant AR interactors in LNCaP cells.

ChIP-seq

ChIPs were performed as described.[14] For details, see Supplementary Materials and Methods. All ChIP-seq data are deposited on NCBI GEO (GSE94682).

Gene expression analysis

Gene expression data from AR-expressing LHSAR normal prostate epithelial cells was downloaded from the NCBI Gene Expression Omnibus database (GSE70078). Gene expression data of The Cancer Genome Atlas PRAD cohort was downloaded from https://xenabrowser.net/ containing the expression data of 496 primary tumor samples and 53 normal samples. Limma R package was used to identify differentially expressed genes between normal and tumor tissue, as well as between LHSAR cells expressing *LacZ* control with cells overexpressing FOXA1 alone, HOXB13 alone or both FOXA1 and HOXB13. Hypergeometric tests were used to test for enrichment of genes of interest in the list of differentially expressed genes. Bonferroni method was used for multiple testing correction.

CONFLICT OF INTEREST

The authors declare no conflict of interest.

ACKNOWLEDGEMENTS

We thank the NKI Genomics Core Facility for Illumina sequencing and bioinformatic support. SS is supported by Movember (NKI01). We thank Corrina MA de Ridder for dedicated maintenance and biobanking of the PDX models. WZ is supported by a KWF Dutch Cancer Society/Alpe d'HuZes Bas Mulder Award (NKI 2014-6711) and a VIDI grant (016.156.401) from The Netherlands Organisation for Scientific Research (NWO). This work is further supported by NWO as part of the National Roadmap Large-scale Research Facilities of the Netherlands, Proteins@Work (184.032.201) to OBB and AFMA and a VIDI grant (723.012.102) to AFMA.

REFERENCES

1 Bolton EC, So AY, Chaivorapol C, Haqq CM, Li H, Yamamoto KR. Cell- and gene-specific regulation of primary target genes by the androgen receptor. *Genes Dev* 2007; **21**: 2005–2017.
2 Heemers HV, Tindall DJ. Androgen receptor (AR) coregulators: a diversity of functions converging on and regulating the AR transcriptional complex. *Endocr Rev* 2007; **28**: 778–808.
3 Huang ZQ, Li J, Sachs LM, Cole PA, Wong J. A role for cofactor-cofactor and cofactor-histone interactions in targeting p300, SWI/SNF and Mediator for transcription. *EMBO J* 2003; **22**: 2146–2155.
4 Yang YA, Yu J. Current perspectives on FOXA1 regulation of androgen receptor signaling and prostate cancer. *Genes Dis* 2015; **2**: 144–151.
5 Jozwik KM, Carroll JS. Pioneer factors in hormone-dependent cancers. *Nat Rev Cancer* 2012; **12**: 381–385.
6 Yu J, Yu J, Mani RS, Cao Q, Brenner CJ, Cao X *et al.* An integrated network of androgen receptor, polycomb, and TMPRSS2-ERG gene fusions in prostate cancer progression. *Cancer Cell* 2010; **17**: 443–454.
7 Wang D, Garcia-Bassets I, Benner C, Li W, Su X, Zhou Y *et al.* Reprogramming transcription by distinct classes of enhancers functionally defined by eRNA. *Nature* 2011; **474**: 390–394.
8 Andreu-Vieyra C, Lai J, Berman BP, Frenkel B, Jia L, Jones PA *et al.* Dynamic nucleosome-depleted regions at androgen receptor enhancers in the absence of ligand in prostate cancer cells. *Mol Cell Biol* 2011; **31**: 4648–4662.
9 van der Steen T, Tindall DJ, Huang H. Posttranslational modification of the androgen receptor in prostate cancer. *Int J Mol Sci* 2013; **14**: 14833–14859.
10 Cross DS, Burmester JK. Functional characterization of the HOXB13 promoter region. *Med Oncol* 2008; **25**: 287–293.
11 Norris JD, Chang CY, Wittmann BM, Kunder RS, Cui H, Fan D *et al.* The homeodomain protein HOXB13 regulates the cellular response to androgens. *Mol Cell* 2009; **36**: 405–416.
12 Kim SD, Park RY, Kim YR, Kim IJ, Kang TW, Nam KI *et al.* HOXB13 is co-localized with androgen receptor to suppress androgen-stimulated prostate-specific antigen expression. *Anat Cell Biol* 2010; **43**: 284–293.
13 Pomerantz MM, Li F, Takeda DY, Lenci R, Chonkar A, Chabot M *et al.* The androgen receptor cistrome is extensively reprogrammed in human prostate tumorigenesis. *Nat Genet* 2015; **47**: 1346–1351.
14 Stelloo S, Nevedomskaya E, van der Poel HG, de Jong J, van Leenders GJ, Jenster G *et al.* Androgen receptor profiling predicts prostate cancer outcome. *EMBO Mol Med* 2015; **7**: 1450–1464.
15 Chen Z, Lan X, Thomas-Ahner JM, Wu D, Liu X, Ye Z *et al.* Agonist and antagonist switch DNA motifs recognized by human androgen receptor in prostate cancer. *EMBO J* 2015; **34**: 502–516.
16 Mateo J, Carreira S, Sandhu S, Miranda S, Mossop H, Perez-Lopez R *et al.* DNA-repair defects and olaparib in metastatic prostate cancer. *N Engl J Med* 2015; **373**: 1697–1708.
17 Asangani IA, Wilder-Romans K, Dommeti VL, Krishnamurthy PM, Apel IJ, Escara-Wilke J *et al.* BET bromodomain inhibitors enhance efficacy and disrupt resistance to AR antagonists in the treatment of prostate cancer. *Mol Cancer Res* 2016; **14**: 324–331.
18 Etani T, Suzuki T, Naiki T, Naiki-Ito A, Ando R, Iida K *et al.* NCL1, a highly selective lysine-specific demethylase 1 inhibitor, suppresses prostate cancer without adverse effect. *Oncotarget* 2015; **6**: 2865–2878.
19 Hsiao JJ, Ng BH, Smits MM, Martinez HD, Jasavala RJ, Hinkson IV *et al.* Research resource: androgen receptor activity is regulated through the mobilization of cell surface receptor networks. *Mol Endocrinol* 2015; **29**: 1195–1218.
20 Hsiao JJ, Smits MM, Ng BH, Lee J, Wright ME. Discovery proteomics identifies a molecular link between the coatomer protein complex I and androgen receptor-dependent transcription. *J Biol Chem* 2016; **291**: 18818–18842.
21 Jasavala R, Martinez H, Thumar J, Andaya A, Gingras AC, Eng JK *et al.* Identification of putative androgen receptor interaction protein modules: cytoskeleton and endosomes modulate androgen receptor signaling in prostate cancer cells. *Mol Cell Proteomics* 2007; **6**: 252–271.
22 Mooslehner KA, Davies JD, Hughes IA. A cell model for conditional profiling of androgen-receptor-interacting proteins. *Int J Endocrinol* 2012; **2012**: 381824.
23 Comuzzi B, Sadar MD. Proteomic analyses to identify novel therapeutic targets for the treatment of advanced prostate cancer. *Cell Sci* 2006; **3**: 61–81.
24 Barfeld SJ, Urbanucci A, Itkonen HM, Fazli L, Hicks JL, Thiede B *et al.* c-Myc antagonises the transcriptional activity of the androgen receptor in prostate cancer affecting key gene networks. *EBioMedicine* 2017; **18**: 83–93.
25 Paltoglou S, Das R, Townley SL, Hickey TE, Tarulli GA, Coutinho I *et al.* Novel Androgen Receptor Coregulator GRHL2 Exerts Both Oncogenic and Antimetastatic Functions in Prostate Cancer. *Cancer Res* 2017; **77**: 3417–3430.
26 Mohammed H, Taylor C, Brown GD, Papachristou EK, Carroll JS, D'Santos CS. Rapid immunoprecipitation mass spectrometry of endogenous proteins (RIME) for analysis of chromatin complexes. *Nat Protoc* 2016; **11**: 316–326.
27 Fang Y, Fliss AE, Robins DM, Caplan AJ. Hsp90 regulates androgen receptor hormone binding affinity in vivo. *J Biol Chem* 1996; **271**: 28697–28702.

28 Fei T, Chen Y, Xiao T, Li W, Cato L, Zhang P *et al.* Genome-wide CRISPR screen identifies HNRNPL as a prostate cancer dependency regulating RNA splicing. *Proc Natl Acad Sci USA* 2017; **114**: E5207–E5215.
29 Massie CE, Adryan B, Barbosa-Morais NL, Lynch AG, Tran MG, Neal DE *et al.* New androgen receptor genomic targets show an interaction with the ETS1 transcription factor. *EMBO Rep* 2007; **8**: 871–878.
30 Wang Q, Li W, Liu XS, Carroll JS, Janne OA, Keeton EK *et al.* A hierarchical network of transcription factors governs androgen receptor-dependent prostate cancer growth. *Mol Cell* 2007; **27**: 380–392.
31 Jia L, Berman BP, Jariwala U, Yan X, Cogan JP, Walters A *et al.* Genomic androgen receptor-occupied regions with different functions, defined by histone acetylation, coregulators and transcriptional capacity. *PLoS ONE* 2008; **3**: e3645.
32 Jangal M, Couture JP, Bianco S, Magnani L, Mohammed H, Gevry N. The transcriptional co-repressor TLE3 suppresses basal signaling on a subset of estrogen receptor alpha target genes. *Nucleic Acids Res* 2014; **42**: 11339–11348.
33 Abrink M, Ortiz JA, Mark C, Sanchez C, Looman C, Hellman L *et al.* Conserved interaction between distinct Kruppel-associated box domains and the transcriptional intermediary factor 1 beta. *Proc Natl Acad Sci USA* 2001; **98**: 1422–1426.
34 Friedman JR, Fredericks WJ, Jensen DE, Speicher DW, Huang XP, Neilson EG *et al.* KAP-1, a novel corepressor for the highly conserved KRAB repression domain. *Genes Dev* 1996; **10**: 2067–2078.
35 Goodwin JF, Schiewer MJ, Dean JL, Schrecengost RS, de Leeuw R, Han S *et al.* A hormone-DNA repair circuit governs the response to genotoxic insult. *Cancer Discov* 2013; **3**: 1254–1271.
36 Haffner MC, Aryee MJ, Toubaji A, Esopi DM, Albadine R, Gurel B *et al.* Androgen-induced TOP2B-mediated double-strand breaks and prostate cancer gene rearrangements. *Nat Genet* 2010; **42**: 668–675.
37 Polkinghorn WR, Parker JS, Lee MX, Kass EM, Spratt DE, Iaquinta PJ *et al.* Androgen receptor signaling regulates DNA repair in prostate cancers. *Cancer Discov* 2013; **3**: 1245–1253.
38 Schiewer MJ, Knudsen KE. Linking DNA damage and hormone signaling pathways in cancer. *Trends Endocrinol Metab* 2016; **27**: 216–225.
39 Schiewer MJ, Goodwin JF, Han S, Brenner JC, Augello MA, Dean JL *et al.* Dual roles of PARP-1 promote cancer growth and progression. *Cancer Discov* 2012; **2**: 1134–1149.
40 Marshall TW, Link KA, Petre-Draviam CE, Knudsen KE. Differential requirement of SWI/SNF for androgen receptor activity. *J Biol Chem* 2003; **278**: 30605–30613.
41 G Hendrickson D, Kelley DR, Tenen D, Bernstein B, Rinn JL. Widespread RNA binding by chromatin-associated proteins. *Genome Biol* 2016; **17**: 28.
42 Bose DA, Donahue G, Reinberg D, Shiekhattar R, Bonasio R, Berger SL. RNA binding to CBP stimulates histone acetylation and transcription. *Cell* 2017; **168**: 135–149 e122.
43 Beltran M, Yates CM, Skalska L, Dawson M, Reis FP, Viiri K *et al.* The interaction of PRC2 with RNA or chromatin is mutually antagonistic. *Genome Res* 2016; **26**: 896–907.
44 Fan S, Goto K, Chen G, Morinaga H, Nomura M, Okabe T *et al.* Identification of the functional domains of ANT-1, a novel coactivator of the androgen receptor. *Biochem Biophys Res Commun* 2006; **341**: 192–201.
45 Goto K, Zhao Y, Saito M, Tomura A, Morinaga H, Nomura M *et al.* Activation function-1 domain of androgen receptor contributes to the interaction between two distinct subnuclear compartments. *J Steroid Biochem Mol Biol* 2003; **85**: 201–208.
46 Boonyaratanakornkit V, Melvin V, Prendergast P, Altmann M, Ronfani L, Bianchi ME *et al.* High-mobility group chromatin proteins 1 and 2 functionally interact with steroid hormone receptors to enhance their DNA binding in vitro and transcriptional activity in mammalian cells. *Mol Cell Biol* 1998; **18**: 4471–4487.
47 Imberg-Kazdan K, Ha S, Greenfield A, Poultney CS, Bonneau R, Logan SK *et al.* A genome-wide RNA interference screen identifies new regulators of androgen receptor function in prostate cancer cells. *Genome Res* 2013; **23**: 581–591.
48 Van Tilborgh N, Spans L, Helsen C, Clinckemalie L, Dubois V, Lerut E *et al.* The transcription intermediary factor 1beta coactivates the androgen receptor. *J Endocrinol Invest* 2013; **36**: 699–706.
49 Le Douarin B, Nielsen AL, Garnier JM, Ichinose H, Jeanmougin F, Losson R *et al.* A possible involvement of TIF1 alpha and TIF1 beta in the epigenetic control of transcription by nuclear receptors. *EMBO J* 1996; **15**: 6701–6715.
50 Zhou XE, Suino-Powell KM, Li J, He Y, Mackeigan JP, Melcher K *et al.* Identification of SRC3/AIB1 as a preferred coactivator for hormone-activated androgen receptor. *J Biol Chem* 2010; **285**: 9161–9171.
51 Vander Griend DJ, Litvinov IV, Isaacs JT. Conversion of androgen receptor signaling from a growth suppressor in normal prostate epithelial cells to an oncogene in prostate cancer cells involves a gain of function in c-Myc regulation. *Int J Biol Sci* 2014; **10**: 627–642.
52 Sahu B, Laakso M, Ovaska K, Mirtti T, Lundin J, Rannikko A *et al.* Dual role of FoxA1 in androgen receptor binding to chromatin, androgen signalling and prostate cancer. *EMBO J* 2011; **30**: 3962–3976.
53 Jin HJ, Zhao JC, Wu L, Kim J, Yu J. Cooperativity and equilibrium with FOXA1 define the androgen receptor transcriptional program. *Nat Commun* 2014; **5**: 3972.
54 van Weerden WM, de Ridder CM, Verdaasdonk CL, Romijn JC, van der Kwast TH, Schroder FH *et al.* Development of seven new human prostate tumor xenograft models and their histopathological characterization. *Am J Pathol* 1996; **149**: 1055–1062.
55 van Weerden WM, Bangma C, de Wit R. Human xenograft models as useful tools to assess the potential of novel therapeutics in prostate cancer. *Br J Cancer* 2009; **100**: 13–18.
56 van Steenbrugge GJ, Groen M, de Jong FH, Schroeder FH. The use of steroid-containing silastic implants in male nude mice: plasma hormone levels and the effect of implantation on the weights of the ventral prostate and seminal vesicles. *Prostate* 1984; **5**: 639–647.
57 Ameziane N, May P, Haitjema A, van de Vrugt HJ, van Rossum-Fikkert SE, Ristic D *et al.* A novel Fanconi anaemia subtype associated with a dominant-negative mutation in RAD51. *Nat Commun* 2015; **6**: 8829.

Supplementary Information accompanies this paper on the Oncogene website (http://www.nature.com/onc)